Rh(I)-complexes of ditopic bis(pyrazol-1-yl)borate ligands: Assessment of their catalytic activity towards phenylacetylene polymerization

Thorsten Morawitz, Songsong Bao, Michael Bolte, Hans-Wolfram Lerner, Matthias Wagner *

Institut für Anorganische Chemie, Goethe-Universität Frankfurt, Max-von-Laue-Straße 7, D-60438 Frankfurt (Main), Germany

ARTICLE INFO

ABSTRACT

Two dinuclear Rh(I)-cyclooctadiene complexes [1,4-(cod)Rh(B(R')pz$_2$)-C$_6$H$_4$-(B(R')pz$_2$)Rh(cod)], linked by a ditopic scorpionate ligand, have been prepared and fully characterized (R' = Ph (**2**), C$_6$F$_5$ (**2^F**); pz = pyrazolide). Both compounds were tested as catalysts for phenylacetylene polymerization but showed no catalytic activity. Attempts at the synthesis of corresponding complexes of the sterically more demanding ligands [1,4-(B(R')pz$_2^{Ph}$)-C$_6$H$_4$-(B(R')pz$_2^{Ph}$)]$^{2-}$ (R' = Ph (**4**), C$_6$F$_5$ (**4^F**); pz^{Ph} = 3-phenylpyrazolide) resulted in B–N bond cleavage and formation of the dinuclear complex [(cod)Rh(μ-pz^{Ph})$_2$Rh(cod)] (**5**). Complex **5** proved to be an efficient catalyst for the preparation of highly stereoregular head-to-tail *cis-trans*oidal poly(phenylacetylene).

1. Introduction

For decades, metal-mediated homogeneous catalysis relied almost exclusively on mononuclear metal complexes as catalytically active species [1], even though numerous metalloenzymes are known in nature for which the added value of a second cooperating metal ion in the active center is clearly proven [2]. Only in the last couple of years reports on bimetallic catalysis have been published which impressively demonstrate that synergistic effects between metal ions can also be achieved in artificially designed oligonuclear systems [3–11].

Our group has a long-standing interest in the development of oligotopic poly(pyrazol-1-yl)borate ("scorpionate" [12,13]) ligands [14–20] that are able to bring two metal ions into sufficiently close proximity so that they can act simultaneously on the same substrate molecule [21–25]. To identify promising applications of ditopic scorpionates of the general formula [1,4-(B(R')pz$_2^R$)-C$_6$H$_4$-(B(R')pz$_2^R$)]$^{2-}$ (pz^R: 3-substituted pyrazolide) in homogeneous catalysis we chose to investigate the Rh-mediated polymerization of phenylacetylene, because (i) mononuclear complexes [(HB(R')pz$_2^{R,R}$)Rh(cod)] (cod: cyclooctadiene) reveal a high activity in this reaction [26], (ii) some benefit of two cooperating metal centers has already been confirmed for homogeneous *olefin* polymerization [27–31], and (iii) stereoregular poly(phenylacetylene) derivatives possess interesting and useful optoelectronic properties [32–38].

The catalytic performance of rhodium scorpionates as phenylacetylene polymerization catalysts is peculiar in several respects [26]. Firstly, both bis- and tris(pyrazol-1-yl)borate complexes of Rh(cod) have been successfully employed, even though in the case of [(HBpz$_3^{R,R}$)Rh(cod)] polymerization is hampered by the fact that an equilibrium exists [39] between the presumed catalytically active κ^2 form and the κ^3 form, which is most likely catalytically inactive. Secondly, the catalytic activity is strongly affected by the substituents R at the 3-positions of the pyrazolyl groups. Thirdly, the polymerization proceeds in a highly stereoregular manner for a variety of different phenylacetylene derivatives to give macromolecules with a head-to-tail *cis-trans*oid structure.

Given this background, we decided to study whether the incorporation of two Rh(cod)-scorpionate complexes into the same catalyst molecule influences the performance of the catalyst and/or the stereoregularity of the polymerization process.

2. Results and discussion

We selected the dinuclear Rh(cod)-complexes **2** and **2^F** (Scheme 1) to assess the impact of the electronegativity of the non-coordinating substituent R' on the stability of the molecular framework and the reactivity of the Rh(I)-ions. Moreover, we wanted to investigate whether the presence of the second Rh-center leads to catalytic activity even though bulky substituents in the 3-positions of the pyrazolyl rings are missing. For a direct comparison of the di- and the mononuclear catalysts it was also necessary to include complexes of the ditopic ligands **4** and **4^F**, bearing sterically demanding 3-phenylpyrazolyl donors, in our study (Schemes 2 and 3).

* Corresponding author. Tel.: +49 69 798 29152; fax: +49 69 798 29260.
E-mail address: Matthias.Wagner@chemie.uni-frankfurt.de (M. Wagner).

1 : R' = Ph
1^F : R' = C$_6$F$_5$

(i) | + Rh$_2$Cl$_2$(cod)$_2$

2 : R' = Ph
2^F : R' = C$_6$F$_5$
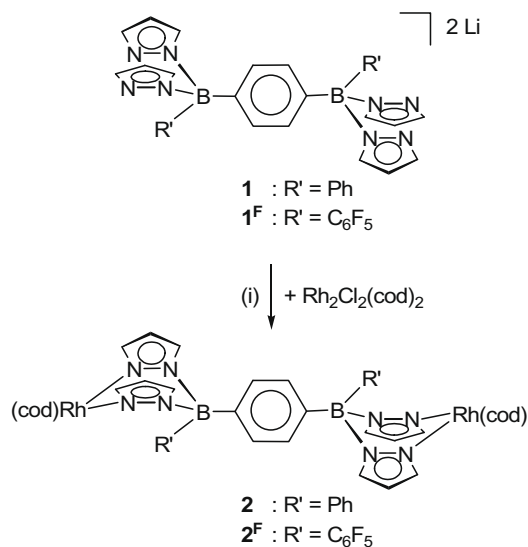
Scheme 1. Synthesis of the dinuclear Rh(cod)-complexes **2** and **2^F**, (i) **2**: r.t., THF; **2^F**: r.t., toluene.

3

(i) | + 2 Kpz^{Ph} / 2 Hpz^{Ph}

4^F
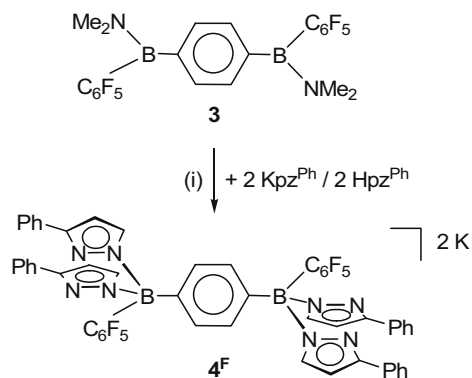
Scheme 2. Synthesis of the sterically demanding ditopic scorpionate ligand **4^F**, (i) r.t., toluene.

2.1. Synthesis and spectroscopical characterization

2 and **2^F** are available in high yield from the reaction of the bis(pyrazol-1-yl)borates **1** [40] and **1^F** [20] with Rh$_2$Cl$_2$(cod)$_2$ (Scheme 1).

The 3-phenylpyrazolyl-substituted scorpionate **4** is already known in the literature [24]. Its partially fluorinated congener **4^F** was synthesized similar to **4** employing the aminoborane **3** [20] and 2 equivalents of a 1:1 mixture of Kpz^{Ph} and Hpz^{Ph} (Scheme 2).

Further treatment of **4** and **4^F** with Rh$_2$Cl$_2$(cod)$_2$ in THF, however, did not give the corresponding Rh^I-complexes but rather led to a multiplicity of products (NMR spectroscopical control) of which the doubly pyrazolide-bridged complex **5** could be isolated and structurally characterized (Scheme 3). These results are remarkable in the light of the successful synthesis of **2** and **2^F** and given the background that the compound [(HBpz$_3^{Ph,Me}$)Rh(cod)], in which a scorpionate ligand with 3-phenyl-5-methylpyrazolyl substituents coordinates to the Rh^I-ion in a κ^2-mode, is also readily accessible [41]. We attribute our failure to prepare Rh^I-complexes of **4** and **4^F** to the facts that bis(pyrazol-1-yl)borate ligands tend to have a lower stability than tris(pyrazol-1-yl)borates [40] and that sterically encumbered poly(pyrazol-1-yl)borates are generally more prone to B–N bond cleavage than less bulky derivatives [13,42].

4 : R' = Ph; M = Li
4^F : R' = C$_6$F$_5$; M = K

(i) | + Rh$_2$Cl$_2$(cod)$_2$

5

(ii) | + 2 Lipz^{Ph}
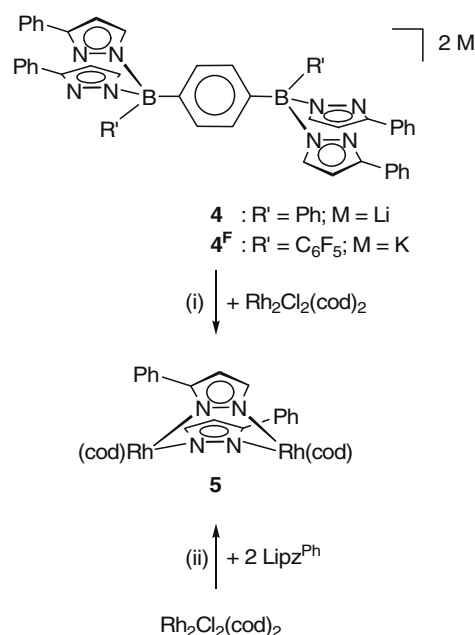
Rh$_2$Cl$_2$(cod)$_2$

Scheme 3. Degradation of **4** and **4^F** by Rh$_2$Cl$_2$(cod)$_2$ to give the dinuclear pyrazolide-bridged complex **5**; targeted synthesis of **5**, (i) r.t., THF; (ii) r.t., toluene.

A targeted synthesis of complex **5** was achieved by reaction of Rh$_2$Cl$_2$(cod)$_2$ with 2 equivalents of Lipz^{Ph} (Scheme 3).

The proton NMR spectra of **2** and **2^F** exhibit only one set of three signals for all four pyrazolyl rings which points towards highly symmetric structures in accord with a successful complexation of *both* bis(pyrazol-1-yl)borate moieties. This interpretation is further supported by the integral values of the scorpionate resonances on one hand and the cyclooctadiene signals on the other (discorpionate:cod = 1:2). The cod-ligands give rise to three multiplets with integral values of 4H, 4H, and 8H in the aliphatic region of the proton spectrum together with two resonances (each integrating 4H) in the typical range of olefinic protons (**2**: δ = 3.68–3.75, 4.01–4.08; **2^F**: δ = 3.69–3.73, 4.35–4.43). The concomitant ^{13}C NMR resonances appear at 30.3, 31.2, 80.9, 81.2 ppm (**2**) and 31.0, 31.2, 82.0, 82.8 ppm (**2^F**); signals belonging to coordinated olefinic carbon atoms are split into doublets due to Rh–C coupling ($^1J_{RhC}$ in the range between 11.9 Hz and 13.0 Hz).

The ^{11}B NMR resonance of the potassium scorpionate **4^F** appears at 0.4 ppm, thereby testifying to the presence of tetra-coordinated boron nuclei [43]. Similar to **2** and **2^F**, all pyrazolyl rings of **4^F** are magnetically equivalent and the 1,4-C$_6$H$_4$ fragment gives rise to one singlet proton resonance. The proton integral ratios confirm the presence of four 3-phenylpyrazolyl fragments *per* 1,4-phenylene linker. Three multiplets at −163.5, −157.3, and −131.5 ppm appear in the ^{19}F NMR spectrum of **4^F**, which is the typical signal pattern of C$_6$F$_5$ substituents in related scorpionates (cf. the ^{19}F NMR spectrum of **1^F**: δ = −167.9, −163.3, −135.8 [20]).

The integral ratio of the 3-phenylpyrazolide rings and the cod-ligands in complex **5** is 1:1. In contrast to **2** and **2^F**, we find 8 cyclooctadiene resonances both in the ^{1}H and in the ^{13}C NMR spectrum of **5**, which is in agreement with an average C_2-symmetric structure similar to the configuration of **5** that has been established by X-ray crystallography (see Fig. 3). However, it has to be mentioned that the NMR data in THF-d_8 would also be in accord with a monomeric solution structure of the form (thf)(pz^{Ph})Rh(cod). For this reason, we have also recorded the ^{1}H NMR spectrum of **5** in the non-coordinating solvent CDCl$_3$ and found an identical signal pattern, which indicates that the dimeric structure of **5** remains intact in solution. Moreover, the mass spectrum of **5** revealed a

peak at $m/z = 708$, corresponding to the molecular mass of the dinuclear species [5]$^+$.

2.2. X-ray crystal structure determinations

The Rh^I-complex 2 crystallizes from THF with two equivalents of non-coordinating THF molecules (2 · 2 THF; Fig. 1, Table 1). In the solid state, the molecule possesses a center of inversion located at the midpoint of the 1,4-phenylene bridge. The two Rh–N bond lengths of 2.091(3) Å and 2.103(4) Å, as well as the distances between the Rh-ions and the centroids (COGs) of the olefinic cyclooctadiene bonds (2.021 Å, 2.028 Å) compare well to the corresponding bond lengths in the mononuclear scorpionate complex [(pzBpz$_3$)Rh^I(cod)] [44]. The most important bond angles about the Rh-ion in 2 · 2 THF are N(12)–Rh(1)–N(22) = 88.7(1)° and COG[C(1)=C(2)]–Rh(1)–COG[C(5)=C(6)] = 87.7°. With respect to the scorpionate ligand, we observe all B–N and B–C bonds in the same range as in the lithium derivative 1 [40]. The most pronounced deviation of a X-B(1)–Y bond angle in 2 · 2 THF from the

ideal value of 109.5° is found for C(31)–B(1)–C(41), which is widened to 114.5(3)°.

Single crystals of the partially fluorinated complex 2^F (incorporating 2 equivalents of CH$_2$Cl$_2$; 2^F · 2 CH$_2$Cl$_2$) were grown from CH$_2$Cl$_2$/hexane at r.t. (Fig. 2, Table 1). Different from 2 · 2 THF, 2^F · 2 CH$_2$Cl$_2$ adopts a conformation with a mirror plane that coincides with the 1,4-phenylene spacer. Moreover, the two C$_6$F$_5$ substituents point into the same direction, while the Ph-rings of 2 · 2 THF are in a trans-arrangement with respect to the B–B-axis. Compared to 2 · 2 THF, there is no significant effect of the electron-withdrawing C$_6$F$_5$ fragments on the B–N, B–C, Rh–N, or Rh–C bonds. The B–C$_6$F$_5$ bonds (1.657(4) Å, 1.662(4) Å), however, are somewhat longer than the B–Ph bonds in 2 · 2 THF (1.618(6) Å). Moreover, the intramolecular distances between the Rh-centers and the ipso-carbon atoms of the aryl substituents are significantly shorter in 2^F · 2 CH$_2$Cl$_2$ (Rh(1)···C(51) = 3.290 Å; Rh(2)···C(41) = 3.169 Å) than in 2 · 2 THF (Rh(1)···C(41) = 3.377 Å). This feature is likely attributable to a weak interaction between the electron-poor C$_6$F$_5$- rings and the charge density localized in the Rh^I-d$_{z^2}$ orbital.
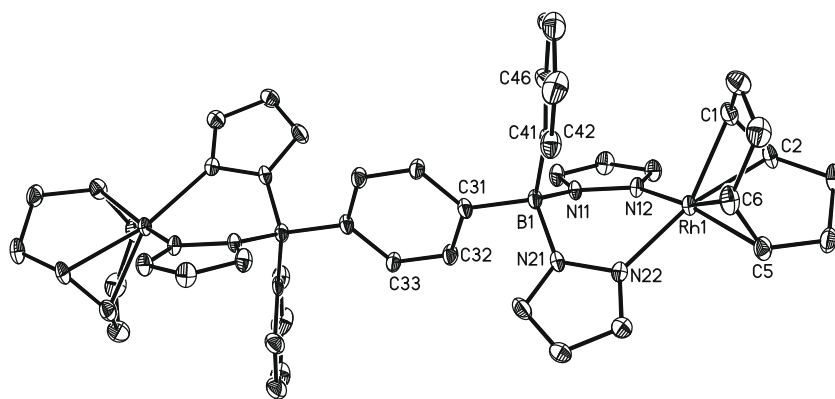

Fig. 1. Structure of 2 · 2 THF in the crystal. Displacement ellipsoids are drawn at the 30% probability level. H atoms and the THF molecules are omitted for clarity. Selected bond lengths (Å), bond angles (°): B(1)–N(11) = 1.573(6), B(1)–N(21) = 1.573(6), B(1)–C(31) = 1.625(6), B(1)–C(41) = 1.618(6), Rh(1)–N(12) = 2.091(3), Rh(1)–N(22) = 2.103(4), Rh(1)–COG[C(1) = C(2)] = 2.028, Rh(1)–COG[C(5) = C(6)] = 2.021; N(11)–B(1)–N(21) = 107.3(3), C(31)–B(1)–C(41) = 114.5(3), N(12)–Rh(1)–N(22) = 88.7(1), COG[C(1) = C(2)]–Rh(1)– COG[C(5) = C(6)] = 87.7.
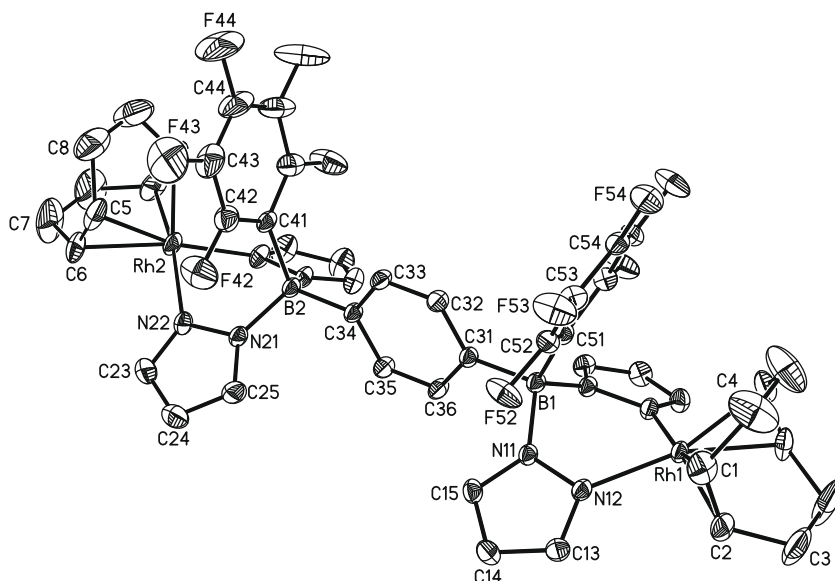

Fig. 2. Structure of 2^F · 2 CH$_2$Cl$_2$ in the crystal. Displacement ellipsoids are drawn at the 30% probability level. H atoms and the CH$_2$Cl$_2$ molecules are omitted for clarity. Selected bond lengths (Å), bond angles (°): B(1)–N(11) = 1.570(2), B(1)–C(31) = 1.620(4), B(1)–C(51) = 1.662(4), B(2)–N(21) = 1.568(3), B(2)–C(34) = 1.625(4), B(2)–C(41) = 1.657(4), Rh(1)–N(12) = 2.098(2), Rh(1)–COG[C(1) = C(2)] = 2.034, Rh(2)–N(22) = 2.097(2), Rh(2)–COG[C(5) = C(6)] = 2.033; N(11)–B(1)–N(11$^#$) = 105.9(2), N(21)–B(2)–N(21$^#$) = 105.4(2), N(12)–Rh(1)–N(12$^#$) = 87.6(1), N(22)–Rh(2)–N(22$^#$) = 86.6(1). $^#$Symmetry transformation used to generate equivalent atoms: x, −y + 1, z.
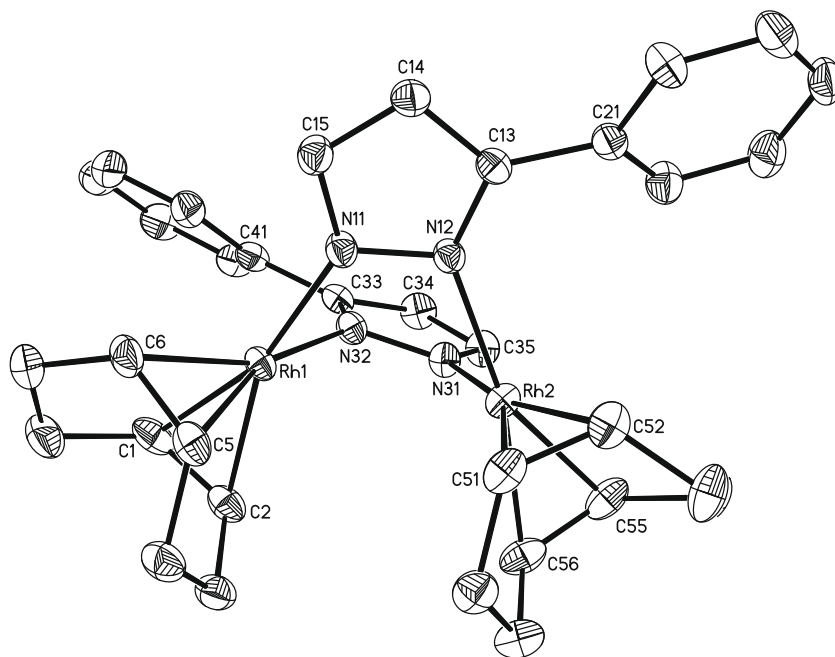
Fig. 3. Structure of **5$_A$** in the crystal. Displacement ellipsoids are drawn at the 50% probability level. H atoms are omitted for clarity. Selected bond lengths (Å), bond angles (°), and torsion angles (°): Rh(1)–N(11) = 2.085(3), Rh(1)–N(32) = 2.116(3), Rh(1)–COG[C(1) = C(2)] = 2.041, Rh(1)–COG[C(5) = C(6)] = 2.021, Rh(2)–N(12) = 2.093(3), Rh(2)–N(31) = 2.079(3), Rh(2)–COG[C(51) = C(52)] = 2.036, Rh(2)–COG[C(55) = C(56)] = 2.018, Rh(1)–Rh(2) = 3.207(1); N(11)–Rh(1)–N(32) = 87.4(1), N(12)–Rh(2)–N(31) = 87.3(1); Rh(1)–N(11)–N(12)–Rh(2) = −17.5(3), Rh(1)–N(32)–N(31)–Rh(2) = −17.2(3).

Two pseudopolymorphs of **5** (**5 · THF/5**) crystallized from the reaction mixtures of **4/4^F** and Rh$_2$Cl$_2$(cod)$_2$, even though the crystallization conditions were rather similar (binary solvent mixture of THF and hexane; r.t.). The asymmetric unit of **5** contains two crystallographically independent molecules **5$_A$** and **5$_B$**. Since the key structural parameters of **5 · THF**, **5$_A$** and **5$_B$** are the same within the experimental error margins, only **5$_A$** is discussed here. The molecular framework of **5$_A$** consists of two Rh^I(cod)-fragments bridged by two 3-phenylpyrazolide ligands in a head-to-tail arrangement (Fig. 3, Table 1).

Both Rh^I-ions are located in a square-planar ligand environment with Rh–N bond lengths ranging from 2.079(3) Å to 2.116(3) Å. The longest bonds are observed for Rh(1)–N(32) = 2.116(3) Å and Rh(2)–N(12) = 2.093(3) Å, which suffer most from the steric repulsion between the cod-ligands and the phenyl rings (the unsubstituted parent compound [(cod)Rh(μ-pz)$_2$Rh(cod)] features Rh–N bond lengths of 2.074(8) Å [45]). The Rh–COG(olefin) distances fall in the interval between 2.018 Å and 2.041 Å. Again, these differences are attributable to different degrees of steric congestion. All in all, no significant differences between the bond lengths and angles about Rh^I are evident in **5$_A$** as compared to **2** or **2^F**. However, we note that the intramolecular Rh–Rh distance of 3.207(1) Å in **5$_A$** is are slightly shorter than in [(cod)Rh(μ-pz)$_2$Rh(cod)] (3.267(2) Å [45]).

2.3. Polymerization reactions

In our initial attempts, we added small quantities of the dinuclear complexes **2** and **2^F** to solutions of phenylacetylene in CH$_2$Cl$_2$. None of these experiments led to the formation of poly(phenylacetylene) (PPA).

We then employed the crude products of the reactions of **4** and **4^F** with Rh$_2$Cl$_2$(cod)$_2$ as phenylacetylene polymerization catalysts. After 24 h at r.t., PPA was obtained in yields exceeding 90%, which is comparable to the results that have been reported for the bis- and tris(pyrazol-1-yl)borate complexes [(H$_2$Bpz$_2^{R,R}$)Rh(cod)] and

Table 1
Selected crystallographic data of **2** · 2 THF, **2^F** · 2 CH$_2$Cl$_2$, and **5**

	2 · 2 THF	**2^F** · 2 CH$_2$Cl$_2$	**5**
Formula	C$_{46}$H$_{50}$B$_2$N$_8$Rh$_2$·2 C$_4$H$_8$O	C$_{46}$H$_{40}$B$_2$F$_{10}$N$_8$Rh$_2$·2 CH$_2$Cl$_2$	C$_{34}$H$_{38}$N$_4$Rh$_2$
Formula weight	1086.59	1292.15	708.50
Color, shape	Light yellow, plate	Light yellow, block	Orange, block
Temperature (K)	173(2)	173(2)	173(2)
Crystal system	Monoclinic	Monoclinic	Triclinic
Space group	$P2_1/c$	$C2/m$	$P\bar{1}$
a (Å)	13.8489(15)	18.6778(7)	13.3910(6)
b (Å)	9.1972(10)	15.3032(7)	14.4836(6)
c (Å)	20.676(3)	18.4775(7)	15.3410(7)
α (°)	90	90	89.883(4)
β (°)	103.502(9)	106.265(3)	87.149(4)
γ (°)	90	90	87.225(3)
V (Å^3)	2560.7(5)	5070.0(4)	2968.2(2)
Z	2	4	4
$D_{calcd.}$ (g cm^{-3})	1.409	1.693	1.585
$F(000)$	1124	2584	1440
μ (mm^{-1})	0.693	0.943	1.142
Crystal size (mm)	0.18 × 0.15 × 0.09	0.52 × 0.48 × 0.46	0.51 × 0.48 × 0.42
Reflections collected	29512	34177	56499
Independent reflections [$R_{(int)}$]	4404(0.0862)	4853(0.0376)	13610(0.0709)
Data/restraints/params	4404/0/308	4853/7/387	13610/0/721
Goodness-of-fit (GOF) on F^2	1.020	1.079	1.157
R_1, wR_2 ($I > 2\sigma(I)$)	0.0426, 0.0990	0.0278, 0.0720	0.0440, 0.1084
R_1, wR_2 (all data)	0.0625, 0.1074	0.0281, 0.0722	0.0461, 0.1096
Largest difference peak and hole (e Å^{-3})	0.614, −0.631	0.491, −0.436	1.320, −1.654

[(HBpz$_3^{R,R}$)Rh(cod)] with sterically demanding substituents R in the 3-positions of the pyrazolyl rings [26]. Our polymeric samples gave well-resolved ^{1}H NMR spectra with resonances at 5.84 ppm

(=CH) and 6.62–6.65/6.92–6.96 ppm (Ph), in excellent agreement with published data for a stereoregular head-to-tail *cis-trans*oidal structure [26]. With respect to the elucidation of the stereostructure of our PPA sample, the vinyl signal at 5.84 ppm is particularly revealing, because it is characteristic to the absorption of a *cis* proton, whereas the vinyl proton in *trans*-poly(phenylacetylene) absorbs at 6.78 ppm [34].

After we had identified complex **5** as one major constituent of the product mixture obtained from **4/4^F** and Rh$_2$Cl$_2$(cod)$_2$, we also examined this compound with regard to catalytic activity. Again, PPA formed in almost quantitative yield after a 24 h reaction time (CH$_2$Cl$_2$, r.t.), and its NMR spectra indicated a very high degree of stereoregularity (head-to-tail, *cis-trans*oidal). A preliminary molecular weight determination using gel permeation chromatography gave values of M_w = 100000 g mol^{-1} and M_w/M_n = 4.6. It is revealing to put the results obtained with **5** in context with a previous report by Ardizzoia on the reactivity of the related Rh^I-complex [Ph$_3$P(C$_2$H$_4$)Rh(μ-dcmpz)$_2$Rh(C$_2$H$_4$)PPh$_3$] (Hdcmpz = 3,5-dicarbomethoxypyrazole) towards phenylacetylene and acetylene [46]. With phenylacetylene as substrate, trimerization reactions to 1,2,4-triphenylbenzene (3%) and 1,3,5-triphenylbenzene (14%) took place, together with the formation of head-to-head dimers (Ph–CC–CH=CH–Ph; 52%) and head-to-tail dimers (Ph–CC–C(Ph)=CH$_2$; 31%). Parent acetylene, however, was polymerized to give a *cis/trans* polyacetylene mixture.

3. Conclusion

The purpose of this paper was to evaluate the potential of dinuclear Rh^I-cyclooctadiene complexes [1,4-(cod)Rh(B(R′)pz$_2^R$)-C$_6$H$_4$-(B(R′)pz$_2^R$)Rh(cod)] as catalysts for the preparation of poly(phenylacetylene) (PPA; R′ = Ph, C$_6$F$_5$; pz^R = pyrazolide, 3-phenylpyrazolide). To this end, we first tested the derivatives **2** (R′ = Ph; R = H) and **2^F** (R′ = C$_6$F$_5$; R = H) which, however, showed no catalytic activity at all. Subsequent attempts at the synthesis of corresponding complexes of the sterically more hindered ligands [1,4-(B(R′)pz$_2^{Ph}$)-C$_6$H$_4$-(B(R′)pz$_2^{Ph}$)]$^{2-}$ (R′ = Ph (**4**), C$_6$F$_5$ (**4^F**)) resulted in the formation of mixtures of several products. These crude mixtures performed very well in the polymerization of phenylacetylene and provided highly stereoregular head-to-tail *cis-trans*oidal PPA. A closer investigation of the catalytically active samples revealed that they contained the 3-phenylpyrazolide-bridged dinuclear species [(cod)Rh(μ-pz^{Ph})$_2$Rh(cod)] (**5**). The formation of **5** requires B-N bond cleavage in **4** and **4^F**. This degradation pathway can obviously not be suppressed by increasing the electronegativity of the substituent R′ (i.e. Ph versus C$_6$F$_5$), but depends to a great extent on the steric bulk of the pyrazolyl rings (i.e. pz versus pz^{Ph}) as evidenced by the successful formation of **2** and **2^F**.

An authentic sample of **5**, prepared from Rh$_2$Cl$_2$(cod)$_2$ and Lipz^{Ph}, showed essentially the same catalytic behavior as the heterogeneous mixture of Rh-compounds described above. This leads to the conclusion that easily accessible dinuclear complexes of type **5** have promising potential for the homogeneous polymerization of phenylacetylene. We are currently studying the influence of the substitution pattern of the pyrazolide bridges on the polymerization kinetics as well as on the structure and the molecular weight distribution of the produced poly(phenylacetylene).

4. Experimental

4.1. General considerations

All reactions and manipulations of air-sensitive compounds were carried out in dry, oxygen-free argon using standard Schlenk ware. CH$_2$Cl$_2$ and CDCl$_3$ were passed through a 4 Å molecular sieves column prior to use. All other solvents were freshly distilled under argon from Na/benzophenone. NMR: Bruker AMX 250, AMX 300, AMX 400, Bruker DPX 250. ^{1}H and ^{13}C NMR shifts are reported relative to tetramethylsilane and were referenced against residual solvent peaks. ^{11}B and ^{19}F NMR shifts are reported relative to external BF$_3$ · Et$_2$O and CFCl$_3$, respectively. Abbreviations: s = singlet, d = doublet, tr = triplet, vtr = virtual triplet, m = multiplet, n. o. = signal not observed, *i* = ipso, *o* = ortho, *m* = meta, *p* = para, pz = pyrazolide, pz^{Ph} = 3-phenylpyrazolide. All NMR spectra were run at room temperature. Elemental analyses were performed by the microanalytical laboratory of the Goethe-University Frankfurt, Germany. Compounds **1** [40], **1^F** [20], **3** [20], and **4** [24] were synthesized according to published procedures.

4.2. Synthesis of **2**

Rh$_2$Cl$_2$(cod)$_2$ (0.148 g, 0.30 mmol) in THF (20 mL) was added to a solution of **1** (0.160 g, 0.30 mmol) in THF (20 mL). The clear yellow mixture was stirred at r.t. for 12 h. All volatiles were removed under reduced pressure and the product was extracted into CH$_2$Cl$_2$ (2 × 40 mL). The extract was evaporated and the solid residue dried in vacuo. Yield of **2** · CH$_2$Cl$_2$: 0.218 g (71%). Single crystals of **2** · 2 THF suitable for X-ray analysis were grown by storing a saturated THF solution at r.t. ^{11}B NMR (96.3 MHz, CDCl$_3$): 2.2 ($h_{1/2}$ = 520 Hz). ^{1}H NMR (300.0 MHz, CDCl$_3$): 1.47–1.53 (m, 4H, cod-CH$_2$), 1.69–1.73 (m, 8H, cod-CH$_2$), 2.22–2.30 (m 4H, cod-CH$_2$), 3.68–3.75, 4.01–4.08 (2 × m, 2 × 4H, cod-CH), 6.15 (vtr, 4H, pzH-4), 6.74–6.79 (m, 4H, Ph), 6.98 (s, 4H, C$_6$H$_4$), 7.23–7.28 (m, 6H, Ph), 7.42, 7.48 (2 × d, 2 × 4H, 2 × $^3J_{HH}$ = 2.1 Hz, pzH-3,5). ^{13}C NMR (75.5 MHz, THF-d_8): 30.3, 31.2 (cod-CH$_2$), 80.9, 81.2 (2 × d, $^1J_{RhC}$ = 12.3 Hz, 12.9 Hz, cod-CH), 104.7 (pzC-4), 126.7, 127.7, 134.4 (Ph), 135.3 (C$_6$H$_4$), 138.1, 140.2 (pzC-3,5), n.o. (CB). Elemental Anal. Calc. for C$_{46}$H$_{50}$B$_2$N$_8$Rh$_2$ [942.37] × CH$_2$Cl$_2$ [84.93]: C, 54.95; H, 5.10; N, 10.91. Found: C, 54.96; H, 5.43; N, 11.15% (the relative amount of CH$_2$Cl$_2$ present in the sample was confirmed by ^{1}H NMR spectroscopy).

4.3. Synthesis of **2^F**

Neat Rh$_2$Cl$_2$(cod)$_2$ (0.237 g, 0.48 mmol) was added to a solution of **1^F** (0.344 g, 0.48 mmol) in toluene (50 mL). The resulting clear yellow solution was stirred at r.t. for 12 h, whereupon a colorless solid precipitated. The precipitate was removed by filtration and the filtrate evaporated to dryness. The solid residue was extracted into CH$_2$Cl$_2$ (2 × 80 mL) and dried in vacuo. Yield of **2^F** · 0.5 CH$_2$Cl$_2$: 0.399 g (71%). X-ray quality crystals of **2^F** · 2 CH$_2$Cl$_2$ were obtained by gas-phase diffusion of hexane into a saturated CH$_2$Cl$_2$ solution. ^{11}B NMR (96.3 MHz, THF-d_8): 0.1 ($h_{1/2}$ = 360 Hz). ^{1}H NMR (300.0 MHz, THF-d_8): 1.76–1.78 (m, 8H, cod-CH$_2$), 1.84–1.93, 2.47–2.56 (2 × m, 2 × 4H, cod-CH$_2$), 3.69–3.73, 4.35–4.43 (2 × m, 2 × 4H, cod-CH), 6.17 (vtr, 4H, pzH-4), 7.29 (s, 4H, C$_6$H$_4$), 7.48, 7.55 (2 × d, 2 × 4H, $^3J_{HH}$ = 2.4 Hz, 2.0 Hz, pzH-3,5). ^{13}C NMR (62.9 MHz, THF-d_8): 31.0, 31.2 (cod-CH$_2$), 82.0, 82.8 (2 × d, $^1J_{RhC}$ = 11.9 Hz, 13.0 Hz, cod-CH), 105.6 (pzC-4), 135.6 (C$_6$H$_4$), 138.0, 141.0 (pzC-3,5), n.o. (CB, CF). ^{19}F NMR (282.3 MHz, THF-d_8): −166.9 (m, 4F, F-*m*), −161.3 (m, 2F, F-*p*), −137.3 (m, 4F, F-*o*). Elemental Anal. Calc. for C$_{46}$H$_{40}$B$_2$F$_{10}$N$_8$Rh$_2$ [1122.24] × 0.5 CH$_2$Cl$_2$ [84.93]: C, 47.95; H, 3.55; N, 9.62. Found: C, 48.28; H, 3.84; N, 9.50% (the relative amount of CH$_2$Cl$_2$ present in the sample was confirmed by ^{1}H NMR spectroscopy).

4.4. Synthesis of **4^F**

A solution of **3** (0.87 g, 1.68 mmol) in toluene (30 mL) was added to a suspension of Kpz^{Ph} (0.61 g, 3.36 mmol) and Hpz^{Ph} (0.48 g, 3.36 mmol) in toluene (20 mL) and stirred at r.t. for 10 h.

The solvent was removed in vacuo and the resulting colorless residue was washed with hexane (50 mL) and dried in vacuo. Yield: 1.28 g (70%). For further purification, the entire product was dissolved in a small amount of THF (5 mL) and precipitated into hexane (30 mL). ^{11}B NMR (96.3 MHz, C_6D_6): 0.4 ($h_{1/2}$ = 590 Hz). ^{1}H NMR (300.0 MHz, C_6D_6): 6.39 (d, 4H, $^3J_{HH}$ = 2.2 Hz, pzH-4), 7.00–7.05 (m, 12H, Ph), 7.40 (s, 4H, C_6H_4), 7.44–7.48 (m, 8H, Ph), 7.74 (d, 4H, $^3J_{HH}$ = 2.2 Hz, pzH-5). ^{13}C NMR (62.9 MHz, C_6D_6): 102.8 (pzC-4), 126.9, 128.5, 129.0 (Ph), 134.0 (C_6H_4), 135.5 (Ph-*i*), 138.3 (pzC-5), 153.9 (pzC-3), n. o. (*C*B, *C*F). ^{19}F NMR (282.3 MHz, C_6D_6): −163.5 (m, 4F, F-*m*), −157.3 (m, 2F, F-*p*), −131.5 (br, 4F, F-*o*). Elemental Anal. Calc. for $C_{54}H_{32}B_2F_{10}K_2N_8$ [1082.63]: C, 59.91; H, 2.98; N, 10.35. Found: a decent elemental analysis was not obtained as a result of varying amounts of coordinated THF and H_2O. However, according to NMR spectroscopy, the ligand was pure and could thus be used for further complexation studies.

4.5. Reaction of **4** with $Rh_2Cl_2(cod)_2$

$Rh_2Cl_2(cod)_2$ (0.094 g, 0.19 mmol) in THF (15 mL) was added to a solution of **4** (0.159 g, 0.19 mmol) in THF (15 mL). After the clear yellow solution had been stirred at r.t. for 18 h, all volatiles were removed under reduced pressure. The ^{1}H NMR spectrum of the solid residue showed a complex mixture of products. Few orange single crystals of **5** · THF were grown by gas-phase diffusion of hexane into a saturated THF solution of the product mixture.

4.6. Reaction of **4^F** with $Rh_2Cl_2(cod)_2$

The reaction was performed similar to the case of **4** and $Rh_2Cl_2(cod)_2$ using $Rh_2Cl_2(cod)_2$ (0.039 g, 0.08 mmol) and **4^F** (0.086 g, 0.08 mmol). Few orange single crystals of **5** were grown by gas-phase diffusion of hexane into a saturated THF solution of the product mixture.

4.7. Synthesis of **5**

Toluene (20 mL) was added to a mixture of neat Lipz^{Ph} (0.066 g, 0.44 mmol) and neat $Rh_2Cl_2(cod)_2$ (0.108 g, 0.22 mmol) at r.t. The resulting pale orange solution was stirred for 18 h. After the solvent had been removed in vacuo the product was extracted into C_6H_6 (40 mL). After filtration, the filtrate was evaporated to dryness. Yield: 0.145 g (93%). Orange crystals of **5** were grown from a saturated THF solution at r.t. by slow evaporation of the solvent. ^{1}H NMR (400.1 MHz, THF-d_8): 1.51–1.60 (m, 2H, cod-CH_2), 1.85–2.00 (m, 4H, cod-CH_2), 2.01–2.13 (m, 4H, cod-CH_2), 2.66–2.76 (m, 4H, cod-CH_2), 2.89–2.99 (m, 2H, cod-CH_2), 3.40–3.44 (m, 2H, cod-CH), 4.05–4.10 (m, 4H, cod-CH), 4.70–4.74 (m, 2H, cod-CH), 6.23 (d, 2H, $^3J_{HH}$ = 2.0 Hz, pzH-4), 7.28 (tr, 2H, $^3J_{HH}$ = 7.8 Hz, Ph-*p*), 7.43 (vtr, 4H, Ph-*m*), 7.49 (d, 2H, $^3J_{HH}$ = 2.0 Hz, pzH-5), 8.29 (d, 4H, $^3J_{HH}$ = 7.4 Hz, Ph-*o*). ^{13}C NMR (100.6 MHz, THF-d_8): 30.1, 31.6, 32.7, 32.9 (cod-CH_2), 78.0, 82.5, 83.2, 83.8 (4 × d, $^1J_{RhC}$ = 11.7 Hz, 11.9 Hz, 13.6 Hz, 11.4 Hz, cod-CH), 104.7 (pzC-4), 127.8 (Ph-*p*), 128.1 (Ph-*o*), 128.8 (Ph-*m*), 136.0 (Ph-*i*), 138.6 (pzC-5), 152.5 (pzC-3). ESI-MS: *m/z* = 708 [**5**]$^+$. Elemental Anal. Calc. $C_{34}H_{38}N_4Rh_2$ [708.50]: C, 57.64; H, 5.41; N, 7.91. Found: C, 57.79; H, 5.43; N, 8.00%.

4.8. Polymerization of phenylacetylene I

0.022 g of the crude product obtained from the reaction of **4** (or **4^F**) with $Rh_2Cl_2(cod)_2$ was dissolved in CH_2Cl_2 (1 mL) at r.t. Phenylacetylene (0.157 g, 1.54 mmol) was added to the yellow solution via syringe, whereupon the reaction mixture immediately turned red. The mixture was stirred for 24 h to complete polymerization. MeOH (30 mL) was added to the viscous liquid to precipitate the

polymer as a yellow powder, which was washed with hexane (2 × 20 mL) and dried in vacuo. Yield: 0.145 g (92%). ^{1}H NMR (250.1 MHz, $CDCl_3$): 5.84 (s, 1H, =CH), 6.62–6.65 (m, 2H, Ph-*o*), 6.92–6.96 (m, 3H, Ph-*m/p*). ^{13}C NMR (75.5 MHz, $CDCl_3$): 126.7 (Ph-*p*), 127.6, 127.8 (Ph-*o,m*), 131.8 (=CH), 139.3 (Ph-*i*), 142.9 (PhC=). IR(KBr, cm^{-1}): $\tilde{v}$ = 3053 (s), 1596 (s), 1489 (s), 1444 (s), 1073 (s), 1028 (s), 882 (br), 753 (shoulder), 737 (s), 695 (s).

4.9. Polymerization of phenylacetylene II

The reaction protocol was the same as above and the polymer obtained showed identical NMR and IR spectra. Amounts employed: **5** (0.040 g, 0.056 mmol), phenylacetylene (0.577 g, 5.65 mmol), CH_2Cl_2 (2 mL). Yield: 0.520 g (90%).

4.10. X-ray crystallography

Data collections were performed on a Stoe IPDS-II two-circle diffractometer with graphite-monochromated Mo Kα radiation. Empirical absorption corrections with the MULABS option [47] in the program PLATON [48] were performed. Equivalent reflections were averaged. The structures were solved by direct methods [49] and refined with full-matrix least-squares on F^2 using the program SHELXL-97 [50]. Hydrogen atoms were placed on ideal positions and refined with fixed isotropic displacement parameters using a riding model.

Compound **2** crystallizes together with two equivalents of non-coordinating THF (**2** · 2 THF). Compound **2^F** crystallizes together with two equivalents of CH_2Cl_2 (**2^F** · 2 CH_2Cl_2). The solvent molecules are disordered over two positions with occupancy factors of 0.53(1) and 0.47(1). In the disordered CH_2Cl_2 molecules, all C–Cl bond lengths on one hand as well as all Cl···Cl distances on the other were restrained to have the same values with an effective esd of 0.02 Å. Compound **5** contains two crystallographically independent molecules in the asymmetric unit (**5$_A$**, **5$_B$**). Although **5** is an achiral compound, **5** · THF crystallizes in a chiral space group and crystals of both enantiomorphous structures have been investigated, i.e. **5**·THF-$P6_5$ and **5** · THF-$P6_1$. The absolute structures have been confirmed by the Flack-x-parameter (−0.07(4) for **5** · THF-$P6_5$; −0.06(3) for **5** · THF-$P6_1$).

Appendix A. Supplementary material

CCDC 691989, 691990, 691991, 691992 and 692179 contain the supplementary crystallographic data for **2** · 2 THF, **2^F** · 2 CH_2Cl_2, **5**, **5** · THF-$P6_5$ and **5**·THF-$P6_1$. These data can be obtained free of charge from The Cambridge Crystallographic Data Centre via www.ccdc.cam.ac.uk/data_request/cif. Supplementary data associated with this article can be found, in the online version, at doi:10.1016/j.jorganchem.2008.09.049.

References

[1] B. Cornils, W.A. Herrmann (Eds.), Applied Homogeneous Catalysis with Organometallic Compounds, A Comprehensive Handbook, Wiley-VCH, Weinheim, 2002.
[2] H.-B. Kraatz, N. Metzler-Nolte (Eds.), Concepts and Models in Bioinorganic Chemistry, Wiley-VCH, Weinheim, 2006.
[3] D.W. Stephan, Coord. Chem. Rev. 95 (1989) 41–107.
[4] M. Sawamura, M. Sudoh, Y. Ito, J. Am. Chem. Soc. 118 (1996) 3309–3310.

[5] A. Schneider, L.H. Gade, M. Breuning, G. Bringmann, I.J. Scowen, M. McPartlin, Organometallics 17 (1998) 1643–1645.
[6] S. Fabre, B. Findeis, D.J.M. Trösch, L.H. Gade, I.J. Scowen, M. McPartlin, Chem. Commun. (1999) 577–578.
[7] E.N. Jacobsen, Acc. Chem. Res. 33 (2000) 421–431.
[8] P. Molenveld, J.F.J. Engbersen, D.N. Reinhoudt, Chem. Soc. Rev. 29 (2000) 75–86.
[9] A. Fukuoka, S. Fukagawa, M. Hirano, N. Koga, S. Komiya, Organometallics 20 (2001) 2065–2075.
[10] B.M. Trost, T. Mino, J. Am. Chem. Soc. 125 (2003) 2410–2411.
[11] A. Ceccon, S. Santi, L. Orian, A. Bisello, Coord. Chem. Rev. 248 (2004) 683–724.
[12] S. Trofimenko, Chem. Rev. 93 (1993) 943–980.
[13] S. Trofimenko, Scorpionates – The Coordination Chemistry of Polypyrazolylborate Ligands, Imperial College Press, London, 1999.
[14] F. Jäkle, K. Polborn, M. Wagner, Chem. Ber. 129 (1996) 603–606.
[15] F. Fabrizi de Biani, F. Jäkle, M. Spiegler, M. Wagner, P. Zanello, Inorg. Chem. 36 (1997) 2103–2111.
[16] S.L. Guo, F. Peters, F. Fabrizi de Biani, J.W. Bats, E. Herdtweck, P. Zanello, M. Wagner, Inorg. Chem. 40 (2001) 4928–4936.
[17] A. Haghiri Ilkhechi, M. Scheibitz, M. Bolte, H.-W. Lerner, M. Wagner, Polyhedron 23 (2004) 2597–2604.
[18] A. Haghiri Ilkhechi, J.M. Mercero, I. Silanes, M. Bolte, M. Scheibitz, H.-W. Lerner, J.M. Ugalde, M. Wagner, J. Am. Chem. Soc. 127 (2005) 10656–10666.
[19] F. Zhang, T. Morawitz, S. Bieller, M. Bolte, H.-W. Lerner, M. Wagner, Dalton Trans. (2007) 4594–4598.
[20] T. Morawitz, M. Bolte, H.-W. Lerner, M. Wagner, Z. Anorg. Allg. Chem. 634 (2008) 1409–1414.
[21] S. Bieller, F. Zhang, M. Bolte, J.W. Bats, H.-W. Lerner, M. Wagner, Organometallics 23 (2004) 2107–2113.
[22] S. Bieller, M. Bolte, H.-W. Lerner, M. Wagner, Inorg. Chem. 44 (2005) 9489–9496.
[23] S. Scheuermann, T. Kretz, H. Vitze, J.W. Bats, M. Bolte, H.-W. Lerner, M. Wagner, Chem. Eur. J. 14 (2008) 2590–2601.
[24] T. Morawitz, M. Bolte, H.-W. Lerner, M. Wagner, Z. Anorg. Allg. Chem. 634 (2008) 1570–1574.
[25] K. Ruth, S. Tüllmann, H. Vitze, M. Bolte, H.-W. Lerner, M.C. Holthausen, M. Wagner, Chem. Eur. J. 14 (2008) 6754–6770.
[26] H. Katayama, K. Yamamura, Y. Miyaki, F. Ozawa, Organometallics 16 (1997) 4497–4500.
[27] L. Li, M.V. Metz, H. Li, M.-C. Chen, T.J. Marks, L. Liable-Sands, A.L. Rheingold, J. Am. Chem. Soc. 124 (2002) 12725–12741.
[28] G.P. Abramo, L. Li, T.J. Marks, J. Am. Chem. Soc. 124 (2002) 13966–13967.
[29] H. Li, L. Li, T.J. Marks, L. Liable-Sands, A.L. Rheingold, J. Am. Chem. Soc. 125 (2003) 10788–10789.
[30] N. Guo, L. Li, T.J. Marks, J. Am. Chem. Soc. 126 (2004) 6542–6543.
[31] J. Wang, H. Li, N. Guo, L. Li, C.L. Stern, T.J. Marks, Organometallics 23 (2004) 5112–5114.
[32] E.T. Kang, P. Ehrlich, A.P. Bhatt, W.A. Anderson, Macromolecules 17 (1984) 1020–1024.
[33] M. Tabata, T. Sone, Y. Sadahiro, Macromol. Chem. Phys. 200 (1999) 265–282.
[34] C.W. Lee, K.S. Wong, W.Y. Lam, B.Z. Tang, Chem. Phys. Lett. 307 (1999) 67–74.
[35] J.C. Salomone, Polymeric Materials Encyclopedia, vol. 8, CRC Press, New York, 1996.
[36] C.-H. Ting, J.-T. Chen, C.-S. Hsu, Macromolecules 35 (2002) 1180–1189.
[37] M. Tabata, Y. Watanabe, S. Muto, Macromol. Chem. Phys. 205 (2004) 1174–1178.
[38] T. Aoki, T. Kaneko, M. Teraguchi, Polymer 47 (2006) 4867–4892.
[39] U.E. Bucher, A. Currao, R. Nesper, H. Rüegger, L.M. Venanzi, E. Younger, Inorg. Chem. 34 (1995) 66–74.
[40] T. Morawitz, F. Zhang, M. Bolte, J.W. Bats, H.-W. Lerner, M. Wagner, Organometallics 27 (2008) 5067–5074.
[41] T. Ruman, Z. Ciunik, A.M. Trzeciak, S. Wołowiec, J.J. Ziółkowski, Organometallics 22 (2003) 1072–1080.
[42] S. Bieller, A. Haghiri, M. Bolte, J.W. Bats, M. Wagner, H.-W. Lerner, Inorg. Chim. Acta 359 (2006) 1559–1572.
[43] H. Nöth, B. Wrackmeyer, Nuclear magnetic resonance spectroscopy of boron compounds, in: P. Diehl, E. Fluck, R. Kosfeld (Eds.), NMR Basic Principles and Progress, Springer, Berlin, 1978.
[44] M. Cocivera, G. Ferguson, B. Kaitner, F.J. Lalor, D.J. O'Sullivan, B. Ruhl, Organometallics 1 (1982) 1132–1139.
[45] K.A. Beveridge, G.W. Bushnell, S.R. Stobart, J.L. Atwood, M.J. Zaworotko, Organometallics 2 (1983) 1447–1451.
[46] G.A. Ardizzoia, S. Brenna, S. Cenini, G. LaMonica, N. Masciocchi, A. Maspero, J. Mol. Catal. A: Chem. 204–205 (2003) 333–340.
[47] R.H. Blessing, Acta Crystallogr. A 51 (1995) 33–38.
[48] A.L. Spek, J. Appl. Cryst. 36 (2003) 7–13.
[49] G.M. Sheldrick, Acta Crystallogr. A 46 (1990) 467–473.
[50] G.M. Sheldrick, SHELXL-97 Structure Solution and Refinement Package, Universität Göttingen, Göttingen, 1997.